Hydroelasticity in Marine Technology 2009
University of Southampton, UK

APPLICATION OF 2D HYDROELASTICITY THEORY TO INVESTIGATE THE FAILURE OF A CONTAINERSHIP

S.H. Miao and P. Temarel
Ship Science, School of Engineering Sciences, University of Southampton, UK

ABSTRACT

This paper focuses on the investigation carried out on the failure of the MSC Napoli using two-dimensional (2D) symmetric (i.e. vertical bending) hydroelasticity analysis. The aim of the investigation was to assess the influence of whipping-induced loads on the structural strength of this containership. Relevant structural, hydrostatic and operational data were provided. The calculations were carried out in head regular and long-crested irregular waves. Both cases included the effect of bottom slamming only. Global wave-induced loads were evaluated along the hull, focusing in particular in the vicinity of the engine room. The investigation showed that whipping, due to bottom slamming, is only important for severe seas. The investigation also showed that the keel stresses, in way of the engine room, can be as large as the keel stresses at amidships.

KEYWORDS

2D hydroelasticity; containership; failure; global loads; global stresses; slamming; whipping

1. INTRODUCTION

In January 2007 the containership MSC Napoli experienced catastrophic failure whilst sailing in the English Channel. A 2D symmetric hydroelasticity analysis was carried out to investigate the influence of whipping-induced loads on the dynamic behaviour of this 4400 TEU containership[1]. This analysis formed part of the investigation by the Marine Accident Investigation Branch (MAIB) into this incident[2].

The main aim of this investigation was to focus on the relevance of the results of hydroelasticity theory in terms of providing an explanation to the causes of the structural failure experienced by this containership. To this end a 2D hydroelasticity analysis was carried out in the frequency domain, in order to establish the fundamentals of the symmetric dynamic behaviour of the containership [3]. Since slamming was the main concern, a time domain investigation of bottom slamming in regular head waves was also undertaken in order to gain a better understanding of the transient response of this vessel in controlled conditions[3,4]. Both of these stages of the investigation also provided the opportunity to assess sensitivity of parameters, such as effective shear area and structural damping. The final stage comprised the time domain symmetric dynamic behaviour in long-crested head irregular waves, defined by wave spectra and including the effects of bottom slamming [5].

The investigation focused in particular on the global wave-induced loads in way of the aft quarter and the engine room (frames 82 and 88), namely the vicinity of the structural failure. The results were obtained in terms of vertical bending moments and direct stresses. The investigation showed that springing was not significant and whipping, due to bottom slamming, is only important for severe seas. The investigation also revealed that the keel stresses, in way of the engine room, can be as large as the keel stresses at amidships.

2. THEORETICAL BACKGROUND

The theoretical background to 2D hydroelasticity is well known[3]. A brief description follows, mainly focusing on the transient response, to familiarize the reader. The equations of motion in regular waves of amplitude *a* and frequency ω, encountered at any heading, are given by:

$$\left[\mathbf{A}(\omega_e)+\mathbf{a}\right]\ddot{\mathbf{p}}(t)+\left[\mathbf{B}(\omega_e)+\mathbf{b}\right]\dot{\mathbf{p}}(t)+\left[\mathbf{C}+\mathbf{c}\right]\mathbf{p}(t)=\boldsymbol{\Xi}(\omega,\omega_e)\exp(-i\omega_e t)\,. \tag{1}$$

In this equation **a**, **b** and **c** represent the (N+1)×(N+1) generalised mass, structural damping and stiffness matrices. **a** and **c** are diagonal and are obtained from the dry hull analysis. **b** is assumed to be diagonal, such that $b_{rr}=2\,\nu_r\,\omega_r\,a_{rr}$, for r>1, where ω_r is the dry hull natural frequency and ν_r is the structural damping factor. **A**, **B** and **C** are the (N+1)×(N+1) generalised added mass, hydrodynamic damping and restoring matrices. The first two are dependent on the encounter frequency ω_e. **Ξ** is the (N+1)×1 excitation vector and is a function of both wave (ω) and encounter frequency. The (N+1)×1 principal coordinate vector **p**(t) is of the form $p_r(t)=p_r\exp(-i\omega_e t)$, with p_r, r=0 (heave), 1 (pitch), 2 (2-node),..N, denoting the (complex) amplitude of the rth principal coordinate. Global wave-induced loads, such as the vertical bending moment at a position x (measured from AP) along the ship are obtained using modal summation, i.e.

$$M(x,t)=\exp(-i\omega_e t)\sum_{r=2}^{N} p_r\,M_r(x)\,. \tag{2}$$

A specified length of forefoot emergence or slamming length l_S results from encounter with a regular head wave of amplitude *a* and frequency ω. The emergence is detected based on the relative motion between the regular head wave and the hull. Subsequently an impingement occurs, namely a bottom slam, with the hull continuing to immerse until it reaches the calm waterline – assumed as the end of slam. Naturally the hull continues to immerse above the calm waterline, but these effects are not accounted here. The transient principal coordinate vector is obtained from:

$$\tilde{\mathbf{p}}(t)=\int_0^t \mathbf{h}(\tau)\;\boldsymbol{\Xi}(t-\tau)\,d\tau \tag{3}$$

where **h** is the impulse response matrix (response to unit impulse) and **Ξ** the transient excitation vector obtained from

$$\boldsymbol{\Xi}(t)=\int_0^{l_S} F_{slam}(x,t)\,\mathbf{w}(x)\,dx \tag{4}$$

where **w** is a vector of mode shapes in the defined slamming length l_S and F_{slam} comprises contributions from bottom impact , as well as rate of change of momentum as the ship immerses following impact[3,4]. It should be noted that slamming forces will also arise from bow flare impact; however, this was not included in the ensuing analysis. The total vertical bending moment, comprising steady state and transient contributions, in regular head waves is

$$M(x,t) = \mathrm{Re}\{\exp(-i\omega_e t) \sum_{r=2}^{N} p_r \, M_r(x)\} + \sum_{r=2}^{N} \tilde{p}_r(t) M_r(x) . \quad (5)$$

The long-crested head irregular sea is generated by combining M regular waves of frequency ω_j and amplitude a_j, based on selected wave spectra, at random phase angles ε_j. The resultant sea elevation along the ship $\zeta(x,t)$ is as follows:

$$\zeta(x,t) = \mathrm{Re}\{\sum_{j=1}^{M} a_j \exp(ik_j x - i\omega_{ej} t - i\varepsilon_j)\} \quad (6)$$

where $k_j=\omega_j^2/g$ is the relevant wave number.

The evaluation of the transient forces and responses are as explained in Eqs.(3 and 4). The steady state part of the simulation is obtained by combining the regular wave responses at random phase angles. The transient response is added after shifting it by t_S, denoting the time elapsed from the start of the record to the start of the slam, i.e. impingement. The total response, for example for the bending moment, is

$$M(x,t) = \sum_{j=1}^{M} \mathrm{Re}\{\exp(-i\omega_{ej} t - \varepsilon_j) \; a_j \sum_{r=2}^{N} p_r \, M_r(x)\} + \sum_{r=2}^{N} \tilde{p}_r(t - t_S) M_r(x) . \quad (7)$$

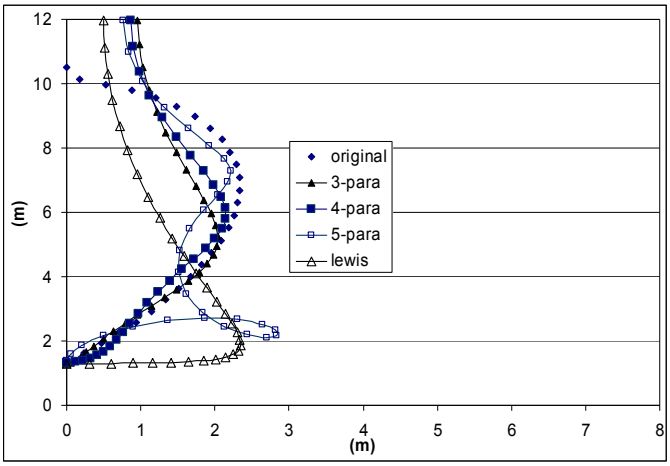

Figure 1: Various conformal transformations for station 50 (0 being A.P., 50 F.P.)

3. SHIP DATA

3.1 Ship Properties

The calculations were based on data supplied for the ship [2]. The 2D idealization was carried using 50 strips along the ship, using the length between perpendiculars L=261.4m and a displacement of 73486 m^3, corresponding to a trimmed condition supplied with draughts at the aft and fore perpendiculars of T_A=13.28m and T_F=11.96m, respectively. The sections were idealized using multi-parameter conformal mapping. The example in Fig.1 shows the difficulties in accurately idealizing station 50 (i.e. FP) accounting for the bulbous bow. In the particular case shown, the 4-parameter idealisation was adopted. The resultant displacement and LCB had an error of less than 0.7% compared to originally supplied data. Data were also supplied for the relevant mass distribution, cross-section area and second moment of area [2]. The effective shear area was

assumed to be in the form of kA, where A denotes the cross-section area and k the effective shear area factor. The keel and deck section moduli are shown in Fig.2, as they are relevant to the discussion of deck and keel stresses in sections 4 and 5.

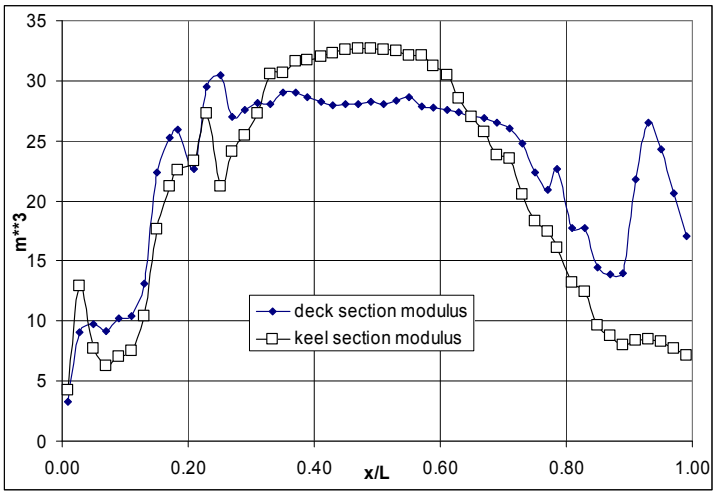

Figure 2: Deck S_d and keel S_k section moduli (m^3) along the ship

3.2 Dry hull natural frequencies

The dry hull analysis was based on a Timoshenko beam theory, ignoring the effects of rotatory inertia. Based on past experience a value of k=0.4 was selected [6,7]. Nevertheless, a limited sensitivity analysis of the effects of effective shear area was carried out using k=0.2. The dry hull natural frequencies for the first five vertical distortions are shown in Table 1. N=6 was shown to be a sufficient number in achieving convergence [2]. Using a value of k=0.4, as can be seen from Table 1, results in small differences for the 2-node natural frequency which has the most significant contribution when evaluating slamming-induced loads. As expected the differences between the two sets of dry hull natural frequencies increase with increasing modal index.

TABLE 1
DRY HULL NATURAL AND WET HULL RESONANCE FREQUENCIES

Modal index (number of nodes)	Natural frequency (rad/s) k=0.2	Natural frequency (rad/s) k=0.4	Wet resonance frequency (rad/s) k=0.4
r=2 (2)	4.97	5.20	3.76
r=3 (3)	10.17	11.38	7.93
r=4 (4)	15.61	18.4	12.57
r=5 (5)	21.45	26.38	--
r=6 (6)	27.65	35.04	--

3.3 Structural damping

The influence of structural damping is very important when evaluating slamming induced loads due to the very small amount of fluid damping at the relatively high frequencies associated with the 2-node wet resonance, hence slamming response [2]. According to the data supplied, the total damping (structural and hydrodynamic) at the 2-node wet resonance was estimated as 1.2% of critical damping, with an estimate of structural damping of the order of 0.8% of critical damping. It practice it is common to adopt Kumai's values for structural damping, scaled to suit a particular type of ship and/or estimates [8]. Using ν_2=0.008, f=3.75 times of Kumai's damping, results in a total damping of 1.5% of critical damping. On the other hand a total damping of 1.2% of critical

damping corresponds to structural damping f=1.61 times that formulated by Kumai [2]. Both of these values were used in the calculation of section 4 in order to assess their influence.

TABLE 2
REGULAR HEAD WAVE AMPLITUDES, RESULTING IN 0.2L EMERGENCE

L/λ	0.8	0.9	1.0	1.1	1.2	1.3	1.4	1.5	1.6
a (m)	9.42	7.92	6.98	6.47	6.39	6.74	7.54	8.65	9.76

4. BEHAVIOUR IN REGULAR WAVES

4.1 Steady state analysis

The calculations were carried out for a forward speed of 5.66 m/s. The wet hull resonance frequencies associated with the distortion modes, for k=0.4, are shown in Table 1. These are approximately 0.7 of the corresponding dry hull natural frequencies. The variation of the vertical bending moment and shear force along the ship, when using k=0.4, for regular wave length λ corresponding to L/λ=1.2 and wave amplitude *a*=6.39m (see Table 2) are shown in Fig.3. These figures show that the steady state bending moment peaks around amidships, whilst the shear force peaks at approximately 0.2L and 0.7L.

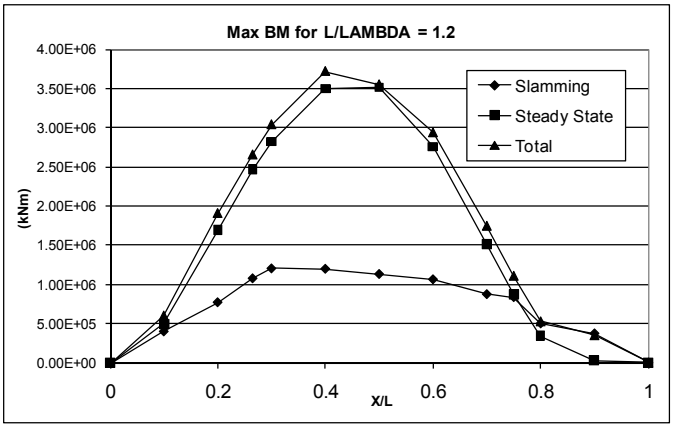

(a)

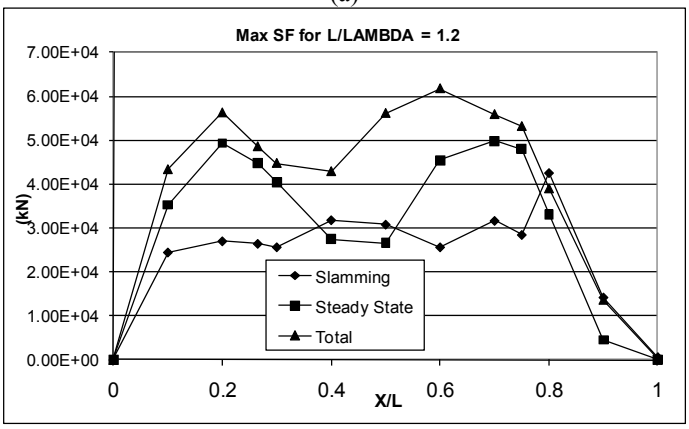

(b)

Figure 3 : Maximum steady state, slamming and total (a) bending moment and (b) shear force along the hull for L/λ=1.2 due to slamming in head regular waves, f=1.61, k=0.4

4.2 Inclusion of bottom slamming

The aim of these calculations is to investigate the influence of two variables, namely structural damping and effective shear area, on the bottom slamming response of the hull. A l_S=0.2L slamming length or forefoot emergence was assumed in the calculations. Accordingly the regular wave amplitude, for a wave of particular frequency ω (or length λ) is obtained such that 0.2L emergence is achieved. These values are shown in Table 2, indicating that the smallest wave amplitudes, of the order of L/40, correspond to wave lengths of the order of ship length. The ensuing impingement, and immersion of the hull, up to the calm water line, defines the slam. The transient forces and corresponding bending moments and shear forces are calculated, as explained in section 2. The slamming length was divided into 10 sections or strips, for evaluating the impact and momentum forces (see Eq.(4)). The relevant stations were placed at x=0.8L, 0.82L, 0.84L, 0.86L, 0.88L, 0.9L, 0.92L, 0.94L, 0.96L and 0.98L, measured from AP.

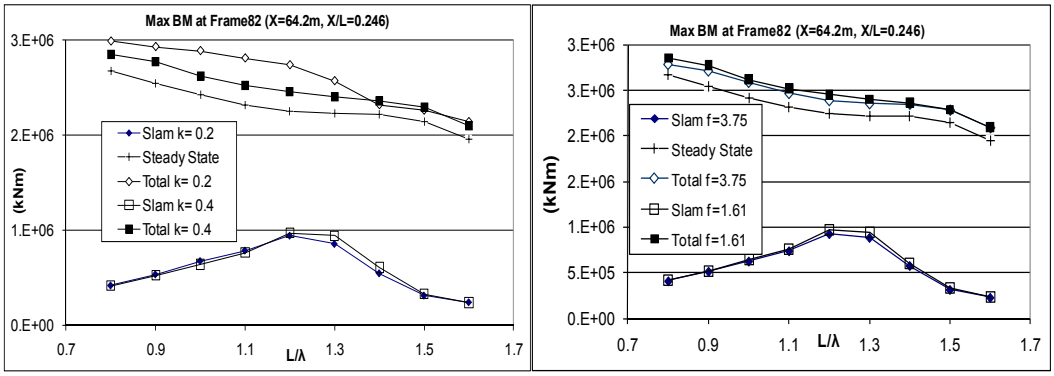

(a) (b)

Figure 4: Maximum steady state, slamming and total bending moments at frame 82 in head regular waves – see Table 2 – (a) influence of effective shear area (k=0.2 and 0.4), structural damping value f=1.61; (b) influence of structural damping (f=1.61 and 3.75), k=0.4

The maximum slamming bending moment at frame 82, calculated from Eq.(5), is shown in Fig.4(a) for different effective shear area factors, k=0.2 and 0.4, when using f=1.61 for structural damping. As can be seen the influence of k is small on the maximum slamming bending moment, with k=0.4 producing slightly higher values. The steady state bending moment is not influenced by the effective shear area in the range of L/λ values used. The total maximum bending moment, also shown in Fig.4(a), produces larger values for k=0.2. This is due to differences in the variation of slamming-induced loads with time (e.g. small differences in wet resonance frequencies) and their phasing with steady state loads, as indicated by Eq.(5). Similar observations can be made, in general, for the loads calculated at frame 88, amidships and the fore quarter [2]. It should be noted that the larger differences for the total bending moment, with different k values, occur at frame 82.

The maximum slamming bending moment at frame 82, calculated from Eq.(5), is shown in Fig.4(b) for different structural damping values, f=1.61 and 3.75, when using k=0.4. As can be seen the influence of structural damping is small with the lower value of f resulting in slightly higher slamming and total maximum bending moment values. The trends are similar for the transient loads at other locations.

It can be seen from Fig.4 that the maximum slamming induced bending moment occurs in the vicinity of L/λ=1.2. Larger values of total bending moment occur at shorter wave lengths. However, these are a result of larger steady state bending moments due to larger wave amplitudes (see Table 2). Based on the aforementioned limited analysis for effective shear area factor and structural damping, values of k=0.4 and f=1.61 are adopted for the subsequent analysis. The maximum slamming and total bending moment and shear force variations along the ship, for

L/λ=1.2, are shown in Fig.3. It can be seen that the influence of slamming only slightly increases the total bending moment. On the other hand slamming has greater influence on the total shear force, especially between 0.4L and 0.6L. The direct stresses at the keel and the deck, corresponding to the maximum slamming and total bending moment values of Fig.3(a) and using the section moduli of Fig.2, are shown in Fig.5 for L/λ=1.2. It is interesting to note in Fig.5 that whilst the deck stresses decrease in the aft half of the ship, from 0.4L towards AP, the keel stresses in the vicinity of the aft quarter are as large as those at amidships. This is the vicinity of frames 82 and 88. This is attributed to the variation of the keel section modulus in Fig.2.

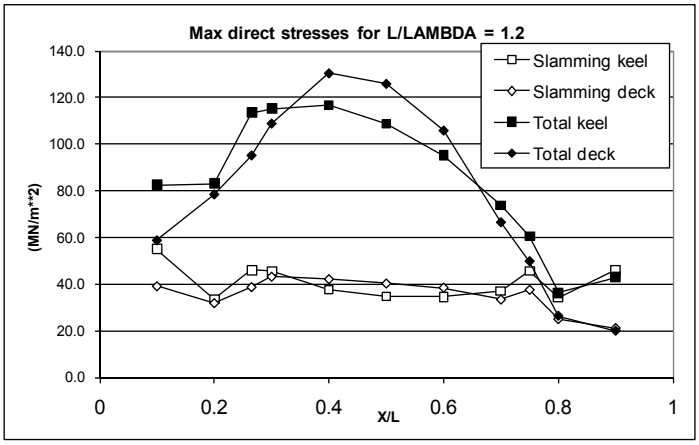

Figure 5: Slamming and total direct stress (MN/m^2) at keel and deck corresponding to bending moments in Fig.3(a)

5. BEHAVIOUR IN IRREGULAR WAVES

5.1 Selection of sea state

The calculations were carried out for the ship travelling at 5.66 m/s in long-crested head irregular waves for two JONSWAP, as well as three ISSC wave spectra [3]. The data for the JONSWAP spectra were supplied as relevant to the environmental conditions the containership operated during the voyage where the accident occurred. These are denoted as Sea1 with significant wave height $h_{1/3}$=7m, average zero crossing period T_z=10s and peak enhancement factor γ=1, and Sea2 with $h_{1/3}$=9m, T_z=11s and γ=5. Several realisations of 30 minute duration were generated for each of these seas using different sets of random phase angles, e.g. Sea11, Sea12, Sea13, Sea14, Sea21, Sea24 etc. The same total slamming length and discretisation outlined in section 4.2 were adopted. Accordingly 0.02L and 0.2L forefoot emergences, define the least and most severe slamming in the simulations. The intensity and severity of slamming varied between the different realisations of the same sea, especially for Sea2. The containership experienced, during the 30 minute simulation, light slamming in Sea1, with just one 0.1L emergence in Sea14 – the most severe case. The slamming was more severe in Sea2, with for example 5 total slams in 30 minutes including one 0.14L emergence in Sea24 – the most severe case. Furthermore the influence of slamming on the bending moment values was relatively small, even in the severe cases. The simulations only account for bottom slamming and do not take into consideration flare slamming which can be quite severe for this type of ship. Therefore, more severe, yet realistic, two-parameter seas were used to increase slamming severity as well as intensity, in an attempt to simulate impulsive forces on the forebody commensurate with severe flare slamming. Accordingly the following two-parameter ISSC wave spectra were selected: Sea3 with $h_{1/3}$=9m and T_z=11s (comparator for Sea2), Sea4 with $h_{1/3}$=10m and T_z=11s and Sea5 with $h_{1/3}$=11m and T_z=11s. In terms of slamming severity and intensity during the 30 minute simulation the ship experienced 6 slams in Sea3 including one 0.06L forefoot emergence (comparable to Sea24), 13 slams in Sea4 including one

0.18L forefoot emergence and 25 slams in Sea5 with 0.2L being the most severe forefoot emergence.

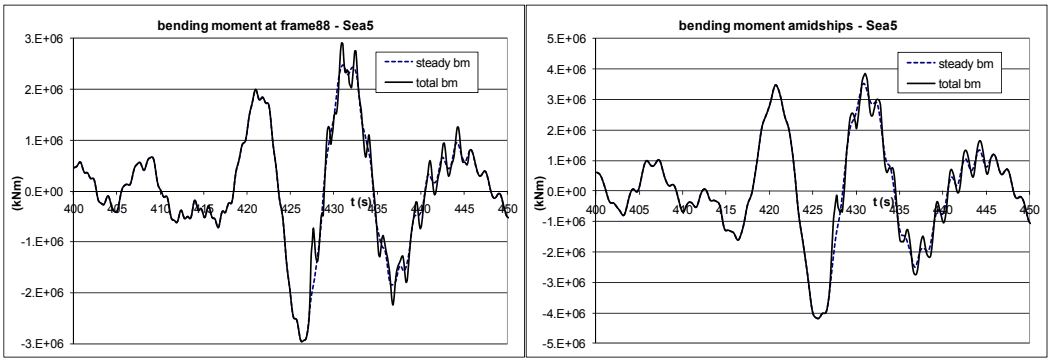

(a) (b)

Figure 6: Portion of bending moment time histories in Sea5 ($h_{1/3}$=11m, T_z=11s) corresponding to the occurrence of a slam with 0.2L forefoot emergence; (a) at frame 82, (b) at amidships

5.2 Analysis of behaviour in irregular waves

A portion of the steady state (excluding slamming) and total bending moment for the containership travelling in Sea5, corresponding to the 0.2L forefoot emergence, is shown in Fig.6 both at amidships and frame 82, where +ve values denote sagging. The simulations show that whipping effects following a slam increase the maximum bending moment for a particular wave encounter. Nevertheless, phasing needs to be taken into account when assessing any increase in the maximum bending moment during a series of wave encounters in irregular seas. Therefore, whipping cannot simply be added to the steady state maximum. This is also valid for the simulations in regular waves in section 4.

TABLE 3
RATIOS OF TOTAL TO STEADY STATE MAXIMUM SAGGING AND HOGGING BENDING MOMENTS

	Sea14	Sea24	Sea25	Sea3	Sea4	Sea5
Amidships - sag	1.01	0.98	1.00	1.03	1.04	1.10
Frame 88 - sag	1.00	1.08	1.00	1.06	1.08	1.17
Frame 82 - sag	1.01	1.08	1.00	1.06	1.08	1.17

To assess the influence of whipping bending moments, the ratios of total to steady state maximum bending moments are shown in Table3, for sagging, at amidships as well as frames 82 and 88 for a range of seas. As can be seen small slamming intensity and severity keeps the ratio at approximately 1 for sagging in Seas 1, 2 and 3, whilst it can reach up to 1.17 (in the vicinity of the aft quarter) for Sea5, the severest of seas. On the other hand for hogging this ratio is 1. It can also be seen that any increase due to slamming is very similar at both frames 82 and 88, and this increase is larger than that at amidships, especially in the severe sea states.

The ratios of maximum total bending moment at frames 82 and 88 to those at amidships are shown in Table 4, both for sagging and hogging, for a range of seas. As can be seen the total maximum sagging bending moments at frames 88 and 82 are approximately 70% and 65%, respectively of that at amidships. These ratios are, in general, higher for more severe seas. The ratios of total maximum direct stresses at frames 88 and 82 to those at amidships, both at keel and deck as well as sagging and hogging, are shown in Table 5. As can be seen whilst the deck stresses at frames 88 and 82 are on average 72% and 61% of those at amidships, respectively, the keel stresses are on average 95% and 90% of those at amidships. Furthermore, although the evidence is limited, increased slamming severity appears to take these ratios closer, and on occasions above, 1 in the vicinity of the aft quarter. These results confirm the distribution of keel stresses observed in Fig.5, for the dynamic behaviour of the containership in regular waves.

TABLE 4
RATIOS OF MAXIMUM TOTAL BENDING MOMENTS AT FRAMES 88 AND 82
TO THOSE AT AMIDSHIPS

	Sea14	Sea24	Sea25	Sea3	Sea4	Sea5
Frame 88 - sag	0.70	0.78	0.61	0.73	0.73	0.75
Frame 88 - hog	0.70	0.68	0.70	0.71	0.71	0.71
Frame 82 - sag	0.64	0.71	0.55	0.66	0.66	0.68
Frame 82 - hog	0.64	0.62	0.63	0.64	0.64	0.64

TABLE 5
RATIOS OF TOTAL MAXIMUM DIRECT STRESSES AT FRAMES 88 AND 82
TO THOSE AT AMIDSHIPS, BOTH KEEL AND DECK

	Sea14	Sea24	Sea25	Sea3	Sea4	Sea5
Frame 88 - keel sag	0.97	1.08	0.85	1.01	1.01	1.05
Frame 88 - keel hog	0.98	0.95	0.98	0.98	0.98	0.98
Frame 88 - deck sag	0.71	0.79	0.62	0.73	0.73	0.76
Frame 88 - deck hog	0.71	0.69	0.71	0.71	0.71	0.71
Frame 82 - keel sag	0.93	1.03	0.79	0.96	0.96	0.99
Frame 82 - keel hog	0.93	0.89	0.92	0.93	0.93	0.93
Frame 82 - deck sag	0.59	0.66	0.51	0.62	0.61	0.64
Frame 82 - deck hog	0.59	0.57	0.59	0.60	0.60	0.60

6. CONCLUSIONS

A 2D hydroelasticity analysis was carried out, including the effects of bottom slamming to find an answer to the question: “Could whipping effects have contributed to the structural failure of this containership?”. In seeking the answer to this question, the analysis also focussed on the influence of structural damping, effective shear area and sea state characteristics, with reference to the effects of whipping. The following conclusions can be drawn:

- Bottom slamming occurs in both of the JONSWAP sea spectra used. It is neither severe nor intense enough for whipping to have any effects in the vicinity of the aft quarter, namely frames 82 and 88.
- More severe, yet realistic, two-parameter seas were used to increase slamming severity as well as intensity, in an attempt to simulate impulsive forces on the forebody commensurate with severe flare slamming, and these produced an increase of up to 17% in the maximum bending moment due to whipping. Whipping will continue to increase with the severity of the seas but this may not correspond to realistic conditions.
- Within the limitations of the 2D investigation carried out, the bending moment and direct stresses due to whipping are not considered significant enough to influence the structural failure in way of frames 82 and 88.
- During the investigations it was observed, with or without the inclusion of slamming, that the keel stresses in the vicinity of the aft quarter, namely frames 82 and 88, can be as large as the keel stresses at amidships. This is an issue of concern, irrespective of the effects of whipping.
- Structural damping values are difficult to establish. Their influence, within the range of the values used, is small and will not affect any conclusions drawn with reference to the influence of whipping.
- Effective shear area values are also difficult to establish. The use of a uniform factor k along the ship can be questioned. Based on limited evidence from this analysis decreasing effective shear area provides a relatively small increase in the bending moments in the vicinity of the aft quarter, namely around frames 82 and 88 – of the order of 10% - due to whipping.

This investigation identified areas where the global 2D analysis may be insufficient in

allowing for the details of the structure around the aft quarter, e.g. influence of effective shear area. Thus, 3D modelling of the structure for global dynamic analysis in waves is recommended, to allow an improved qualitative, as well as quantitative, understanding of the wave-induced stress distribution in the vicinity of the aft quarter[6,7].

Furthermore it is important to simulate flare slamming and its consequent stresses. This can be carried out within the 2D hydroelasticity analysis by extending existing methodology that accounts for the flare influence as a continuation of the bottom slamming process [9]. It can also be investigated within the 3D hydroelasticity analysis through extension of the work carried out for slamming of trimarans [10].

ACKNOWLEDGEMENTS

The authors are grateful to Marine Accident Investigation Branch (MAIB), UK and Det Norske Veritas (DNV) for their support during the investigations.

REFERENCES

1. MAIB, Report on the investigation of the structural failure of MSC Napoli English Channel on 18 January 2007. *Marine Accident Investigation Branch*, UK, 2008, Report 8.
2. WUMTIA, Whipping calculations on the MSC Napoli: 2D hydroelasticity calculations. *Wolfson Unit for Marine Technology & Industrial Aerodynamics*, 2007, Report 2014.
3. Bishop, R.E.D. and Price, W.G., *Hydroelasticity of Ships*, Cambridge University Press, 1979.
4. Belik, O., Bishop, R.E.D. and Price, W.G., On the slamming response of ships to regular head waves. *Trans. Royal Institution of Naval Architects*, 1980, 122, 325-337.
5. Belik, O., Bishop, R.E.D. and Price, W.G., A simulation of ship responses due to slamming in irregular head waves. *Trans. Royal Institution of Naval Architects*, 1983, 125, 237-253.
6. Price, W.G., Salas Inzunza, M. and Temarel, P., The dynamic behaviour of a mono-hull in oblique waves using two- and three-dimensional fluid structure interaction models. *Trans. Royal Institution of Naval Architects*, 2002, 144, 1-26.
7. Hirdaris, S.E., Price, W.G. and Temarel, P., Two- and three-dimensional hydroelastic modelling of a bulker in waves. *Marine Structures*, 2002, 16, 627-658.
8. Betts, C.V., Bishop, R.E.D and Price, W.G., A survey of internal hull damping. *Trans. Royal Institution of Naval Architects*, 1977, 119, 125-142.
9. Belik, O., Bishop, R.E.D. and Price, W.G., Influence of bottom and flare slamming on structural responses. *Trans. Royal Institution of Naval Architects*, 1988, 130, 261-275.
10. Miao, S.H., Temarel, P. and Hampshire, J.K., Dynamic loads on a trimaran travelling in irregular seaways, including slamming. *Proc. 3rd Int. Conf. Hydroelasticity in Marine Technology*, 2003, 185-194, Oxford, UK.